MANSOURA JOURNAL OF CHEMISTRY
Official Journal of Faculty of Science, Mansoura University, Egypt
E-mail: scimag@mans.edu.eg ISSN: 2974-4938

Synthesis, Characterization, Computational Studies and Biological Potency of Novel Zn(II) and Pb(II) Complexes of Carbothioamide Derivative.

Asmaa W. Abo El-Ata[1], Mohammed M. El-Gamil[1,2], Samira M. Abozeid[1,3],Gaber M. Abu El-Reash[1*]

[1]*Department of Chemistry, Faculty of Science, Mansoura University, El-Gomhoria Street, 35516 Mansoura, Egypt*

[2]*Department of Toxic and Narcotic Drug, Forensic Medicine, Mansoura Laboratory, Medico legal Organization, Ministry of Justice, Mansoura, Egypt*

[3]*Chemistry Department, Faculty of Science, New Mansoura University, New Mansoura City, Egypt*

**** Correspondence to:*** *gaelreash@mans.edu.eg, 01000373155*

Received:12/1/2025
Accepted: 27/1/2025

Abstract: Novel series of Zn^{2+} and Pb^{2+} complexes derived from *(Z)-2-(2-oxoindolin-3-ylidene)-N-phenylhydrazine-1-carbothioamide* (H_2L^1). IR,UV-vis, thermal (TGA DrTGA), and elemental (CHN) analyses were used to synthesize and analyze Zn^{2+} and Pb^{2+} complexes . DMol^3 tool of the material studio program was utilized to obtain the optimized structures of the H_2L^1 ligand besides the prepared complexes. In both complexes, the ligand acts as a mononegative ONS tridentate. HOMO, LUMO, bond angles, bond lengths, and dipole moment were computed from the modeling studies to validate the geometry of the ligand beside that its studied chelates. They estimated the different kinetic and thermodynamic parameters using Horowitz–Metzger and Coats–Redfern methods. The thermal analyses demonstrated both thermal decomposition occurred for the metal chelates and the kind of water molecules that are a part of them. Finally, the antioxidant and antimicrobial studies of the tested chelates were also evaluated.

keywords: Thiosemicarbazone, DFT, TGA , and antioxidant activity

1.Introduction

Schiff bases are imine or azomethine(C=N) Compounds frequently synthesized through the condensation of primary amines with aldehydes or ketones can effectively form stable complexes with metal ions, especially transition metals [1, 2]. A notable subset of these compounds, thiosemicarbazones, falls under the category of Schiff bases and contains S, N-donor ligands [3]. For several decades, people have been greatly interested in the synthesis of thiosemicarbazones (TSCs) derivatives and their metal complexes due to their various biological activities, such as anticancer [4, 5] , antibacterial , antimicrobial , anticancer effects , antiparasitic , anti-HIV, antimalarial, antidepressant, antiprotozoal, antiviral drugs, antifungal drugs , antioxidants, antidiabetic drugs[6, 7] etc... Metal complexes always have more biological activities than free ligands. Of all the metal, Transition metals, due to their variable oxidation states, are frequently utilized in medicinal chemistry. Metal-involved syntheses is often favored because metal centers can activate reactants, resulting in fewer steps to produce the target compound [8]. Ligands that include donor atoms such as O, N, S, and P are found to be the most effective in therapeutics[9] . Isatins (1H-indole-2,3-dione) are an important class of heterocyclic compounds due to their diverse biological properties such as antitumor, antibacterial ,anti-inflammatory, analgesic, anti-mycobacterial, anticonvulsant, antiviral, anthelmintic, anti-HIV, antioxidant and central nervous system depressant effects [10]. We use Zinc ions, recognized as the second most prevalent transition metal ions within the human body, are essential for the catalytic activity of numerous enzymes and for the process of gene transcription. In biological systems, the

majority of zinc ions are securely attached to proteins, serving critical structural and catalytic roles. Also , Lead and its compounds have been used in a variety of household items, including paints, ceramics, plumbing materials, solders, gasoline, batteries, ammunition, and cosmetics. Consequently, these past and present uses can lead to the release of lead into the environment.

Therefore, This work's objective is to describe. the synthesis and clarify the structure of a new thiosemicarbazone named *(Z)-2-(2-oxoindolin-3-ylidene)-N-phenylhydrazine-1-carbothioamide*) (H_2L^1) and its Zn^{2+} and Pb^{2+} . Also the investigation of the antioxidant and antimicrobial properties within the title compounds.

2. Materials and Instrumentation

All solvents and chemicals utilized were acquired from reputable suppliers such as Merck and Sigma-Aldrich. Infrared spectra were recorded using a Mattson 5000 FTIR Spectrophotometer within the range of (4000 – 400 cm^{-1}) , utilizing KBr discs. Carbon, hydrogen, and nitrogen contents were conducted using a Perkin-Elmer 2400 Series II analyzer. Metal contents of the complexes were determined through standard gravimetric methods[11] . The Spectrophotometer (ATI UNICAM UV–Visible UV2) was employed to acquire electronic spectra. Thermogravimetric measurements (TGA, DTG, 20–900 °C) were carried out on a DTG-50 Shimadzu thermogravimetric analyzer with a rate of heating (10 °C/min) with a nitrogen flow rate of 20 ml/min. All measurements were performed at room temperature.

2.1. Preparation of ligand

Thiosemicarbazone derivative (H_2L^1) was synthesized and analyzed as detailed in our previously paper [12]. An equimolar amount of isatin with thiosemicarbazide (4-Phenyl thiosemicarbazide) was refluxed with stirring in ethanol for 4 hr. Hot ethanol, diethylether and a desiccator over anhydrous $CaCl_2$ were used to filter and wash the reflux-forming precipitates.

2.2. Synthesis of complexes:

A hot ethanolic solution of solid ligand *(Z)-2-(2-oxoindolin-3-ylidene)-N-phenylhydrazine-1-carbothioamide*) (1 mmol) was refluxed with 1 mmol of $Zn(CH_3COO)_2.2H_2O$, or $Pb(CH_3COO)_2$ salts dissolved in dist H_2o at 80 °C for 4 hours in presence of stirrer , the precipitate was then isolated, filtered, washed, dried and stored in an anhydrous $CaC1_2$ vacuum desiccator. Zn^{2+}complex (1) is orange color, with 90% yield, m.p over 300˚C, M.F. = $C_{17}H_{14}N_4O_3SZn$, M.W. = 419.76 g/m, found (calculated) elemental analysis C= 48.35 (48.64), H= 3.20 (3.36), N= 12.95 (13.35), S= 7.45 (7.64), and Zn= 15.40 (15.58). Pb^{2+} complex (2) is orange color, with 83 % yield, m.p.= 242- 244 ˚C, M.F. = $C_{17}H_{18}N_4O_5PbS$, M.W. = 597.61 g/m, C= 33.90 (34.17), H= 3.01 (3.04), N= 9.25 (9.38), S= 4.98 (5.36), and Pb= 34.10 (34.67).

2.3. Biological applications

2.3.1. Antimicrobial activity

The evaluation of the antimicrobial properties of the ligand H_2L^1 , Zn(II) and Pb(II) chelates were conducted through agar diffusion technique [13, 14]. *Salmonella typhi* (*sal.typho*) and *Escherichia coli* (*E.coli*) utilized for instance of *Gram-negative* bacteria , and *Bacillus subtilis* (*B. st*) also *Staphylococcus Pasteuri* (*S. pas*) just like *Gram-positive* bacteria. As a negative control, DMSO was used, while Gentamicin served as a standard antibiotic. Gentamicin's antibacterial activity was assessed utilizing the previously method and solvent as mentioned before. The effectiveness of Gentamicin was detected by calculating the inhibitory zone diameter´s .The percent activity index of the chelates was calculated [15].

2.3.2. Antioxidant activity using DPPH assay:

The antioxidant capacity of investigated compounds was assessed utilizing the DPPH• colorimetric method with standard ascorbic acid, as reported[16]. The electron donor capacity of the examined compounds was measured by reducing a stable DPPH free radical, changing its color from purple to yellow diphenyl picryl hydrazine. Stock samples were dissolved in n 7 mg/ml DMSO, and their absorbance was measured at 517 nm.

3. Results and Discussion

Table 1 summarize the molecular formulas, elemental analysis, and some of the physical

characteristics of H_2L^1 , Zn(II) and Pb(II) complexes. The produced complexes are soluble in DMF and DMSO but non-hygroscopic and insoluble in water besides that outperforming solvents.

Table 1: Physical and analytical data of ligand and metal complexes

Compound molecular formula	(F.Wt)	color	M.P. (^oC)	Found (calcd.)%				yield %
				M	C	H	N	
H_2L^1 $C_{15}H_{12}N_4OS$	296.35	Yellow	233-235	–	60.04 (60.79)	4.09 (4.08)	18.5 (18.91)	85
$[Zn(HL^1)(OAC)]$ $C_{17}H_{14}N_4O_3SZn$	419.76	Orange	>300	15.40 (15.58)	48.35 (48.64)	3.20 (3.36)	12.95 (13.35)	90
$[Pb(HL^1)(H_2O)_2(OAC)]$ $C_{11}H_{15}ClPtN_4O_3S$	597.61	Orange	242-244	34.10 (34.67)	33.90 (34.17)	3.01 (3.04)	9.25 (9.38)	83

3.1. IR Spectra:

Table 2 indicates to the main IR bands of investigated compounds. In $[Zn(HL^1)(OAC)]$ complex (Figure 1), H_2L^1 ligand behaves as mononegative ONS tridentate via O atom of C=O, N of $(C=N)_{azomethine}$. and S of C=S. Weakness and a slight shift of bands ascribed to υ(C=O) and$(C=N)_{azomethine}$ to lower wavenumber and increase in υ(N-N) bands to high wavenumbers, indicates sharing of free ligand in coordination via azomethine nitrogen atom to Zn (II) atom.

In $[Pb(HL^1)(H_2O)_2(OAC)]$ complex (Figure 1), the ligand binds the metal ion in mononegative as NOS tridentate through O atom of C=O, N of $(C=N)_{azomethine}$ and S of C=S. The disappearance of υ $(NH)_c$ band indicating loss of hydrogen from the nitrogen which is supported by a positive shift in υ (N–N) [17] with the concurrent emergence of new azomethine band at 1617 cm^{-1} in Pb(II) complex.

The shift of thioamide bands (I)-(IV) in all complexes may demonstrate the bonding via (CS) group in thiol form. The presence of

acetate group in $[Zn(HL^1)(OAC)]$ and $[Pb(HL^1)(H_2O)_2(OAC)]$ complexes in coordination sphere is supported by the bands at 1558-1541 and 1456-1441 cm^{-1} assigned to ν_{as}(OCO) and ν_s(OCO) vibrations,respectively, attributable to monodentate acetate vibrations . The acetate group is monodentate, as seen by the frequency difference (Δv= 102, 100 cm^{-1}, respectively).[18, 19]

3.2. Electronic spectra :

The electronic spectral features of the metal complexes in DMSO. The spectrum of diamagnetic $[Zn(HL^1)(OAC)]$ complex, results in a little change in the energy of bands due to the n → π* and π → π*transitions. Also, the broad band at 21505 cm^{-1} (465 nm) is due to LMCT [16] . The spectrum as well as the diamagnetic behavior suggests structure Figure 2.

The spectrum of diamagnetic $[Pb(HL^1)(H_2O)_2(OAC)]$ complex , results in a little change in the energy of bands due to the n → π* and π → π*transitions. Also, the broad band at 20920 cm^{-1} (478 nm) is due to LMCT. The spectrum as well as the diamagnetic behavior suggests structure Figure 2.

Table 2: IR bands of H_2L^1 and its complexes.

Compound		H_2L^1	$[Zn(HL^1)(OAC)]$	$[Pb(HL^1)(H_2O)_2(OAC)]$
$\nu(NH)^a$		3296	3251	3215
$\nu(NH)^b$		3247	3189	3178
$\nu(NH)^c$		3176	–	-
$\nu(C=N)_{az}$		1619	1601	1594
ν(C=O)		1692	1687	1677
δ (C=N)		656	612	611
ν(N-N)		1030	1045	1040
Thioamide	(I)	1465	1406	1441
	(II)	1346	1316	1316
	(III)	1145	1167	1178
	(IV)	795	779	786
δ(C-S)		–	661	653
$\nu(C=N)^*$		–	1611_{sh}	1617

Sh: Shoulder

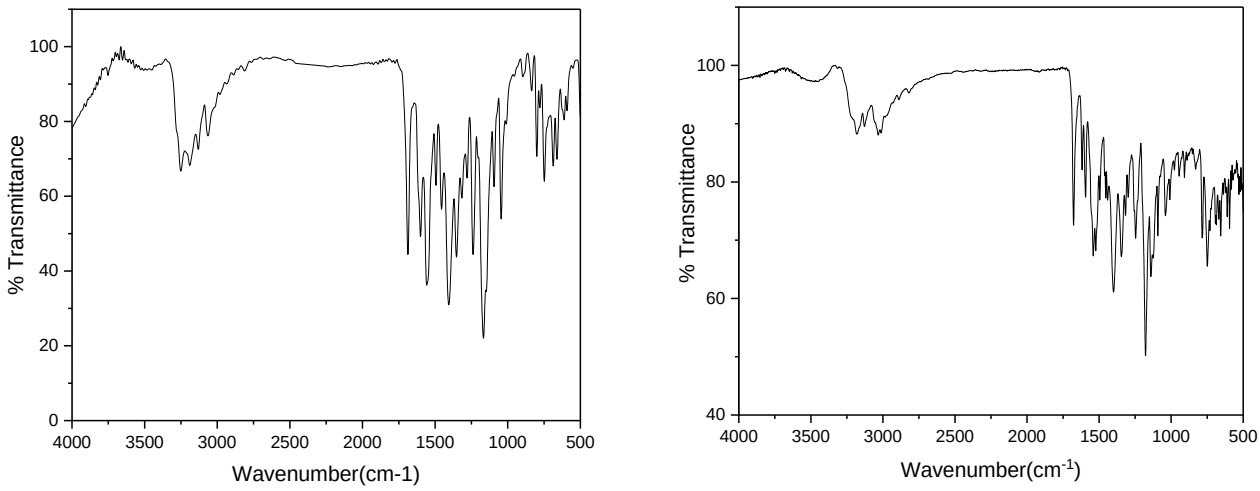

Zn(II)-complex **Pb(II)-complex**

Figure 1: FT-IR Spectrum of Zn(II) and Pb(II)Complexes

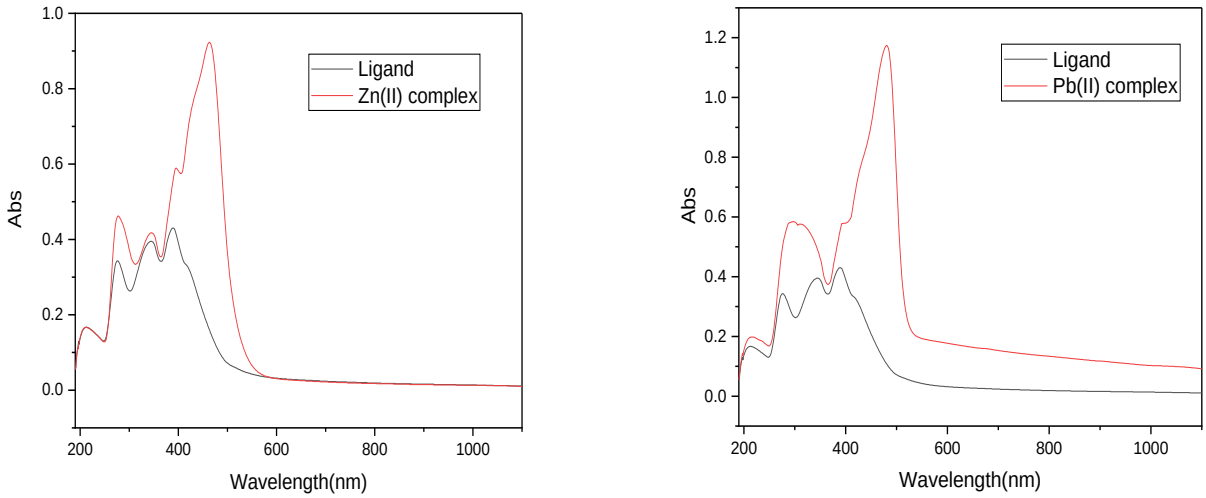

Zn(II)-complex **Pb(II)-complex**

Figure 2: UV-vis. Spectra in DMSO of **Zn(II)** and **Pb(II)** complexes

3.3. Thermogravimetric & Kinetic Data Analysis

Table 3 displays all data, including breakdown steps, temperature ranges, loss of weight percentages and breakdown products for the existing metal complexes , as well as their TGA curves are graphically shown in Figure 3 (Kinetic data showing in Tables 4,5 and Figures 4 -7) .TG (thermogram) of Zn(II) (Figure 3), the first decomposition step for instance, takes place at (271-392°C) with loss of weight (found: 57.12%; Calcd. 57.65%) indicating to the elimination of $C_{12}H_{10}O_2$+2N_2 fragments. The second step (392-560°C) with loss of weight (found: 24.01%; Calcd. 23.82%) is due to elimination of C_4H_4OS fragments . The final step was for the residue. Included loss of Zn+C in weight loss (found: 18.87%; Calcd. 18.43%) at temperature range of 560-900°C.

Key observations from the data analysis (**Error! Reference source not found.** 4 and 5) include:

i. The estimated values for E, A, ΔH^*, ΔS^*, and ΔG^* are consistently comparable across all studied complexes.

ii. A first-order decomposition model (n=1) was validated using both methods.

iii. Positive ΔG^* values indicate a decreasing rate of ligand removal with additional decomposition steps, reflecting increased structural rigidity in the residual complex due to ligand removal [20, 21].

iv. Positive ΔS^* values suggest increasing disorder as decomposition progresses [22]. Activated fragments exhibit a more ordered structure compared to undecomposed fragments, leading to delayed degradation

reactions, as indicated by negative entropy of activation (ΔS^*) values for certain decomposition phases in metal complexes [23].

v. All decomposition processes exhibit endothermic behavior, as evidenced by positive ΔH^* values.

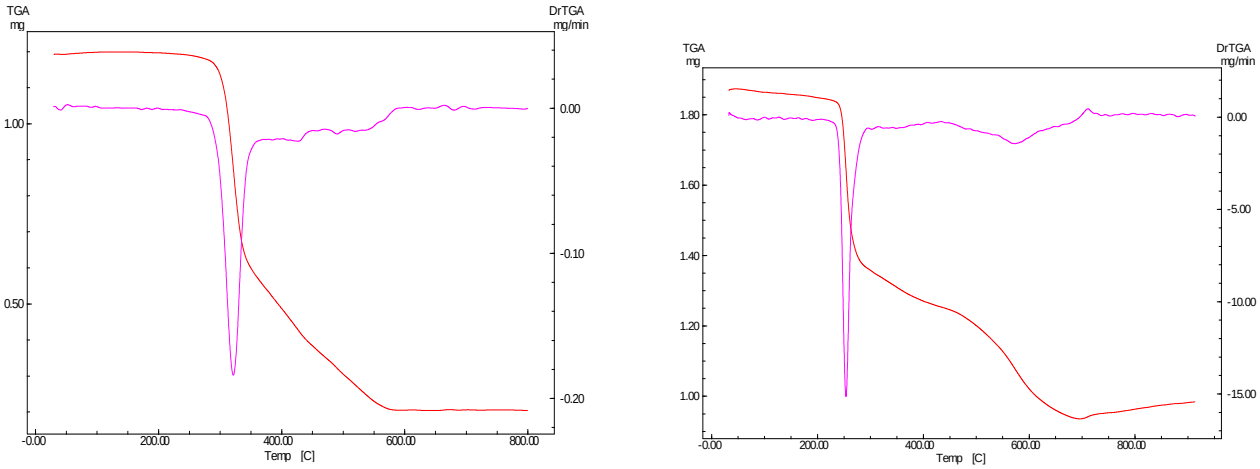

Zn(II)-complex **Pb(II)-complex**

Figure 3: (TGA, DrTGA) curves of Zn(II) and Pb(II) complexes.

Table 3: Decomposition steps for the metal complexes.

Compound	Temp. Range,˚C	Removed species	Wt.Loss	
			Found%	Calcd%
$[Zn(HL^1)(OAc)]$ **(1)** **$C_{17}H_{14}N_4O_3SZn$**	271-392	$-(C_{12}H_{10}O_2+2N_2)$	57.12	57.65
	392-560	$-(C_4H_4OS)$	24.01	23.82
	560-900	(Zn +C)	18.87	18.43
$[Pb(HL^1)(H_2O)_2(OAc)]$ **(2)** **$C_{17}H_{18}N_4O_5PbS$**	130-296	$-(2H_2O+C_2H_5S+N_2+NH_4OH)$	26.73	26.77
	296- 413	-(NO)	5.25	5.02
	413-759	$-(C_8H_4)$	16.60	16.70
	759-900	(PbO+7C)	51.42	51.37

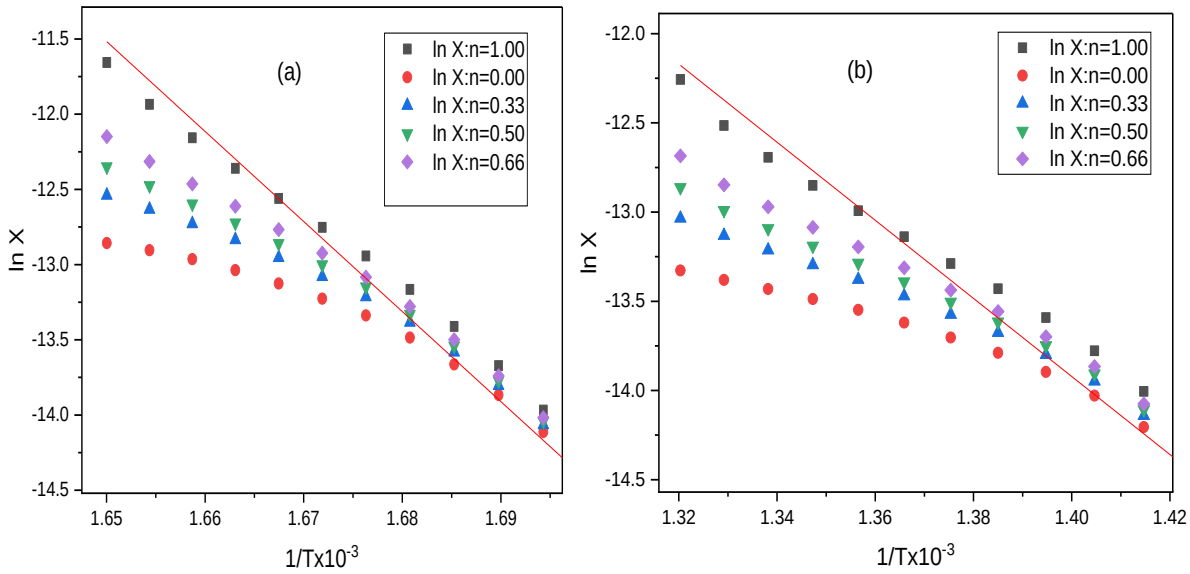

Figure 4 : Coats-Redrern plots of (a) first and (b) second degradation steps for $[Zn(HL^1)(OAc)]$ complex

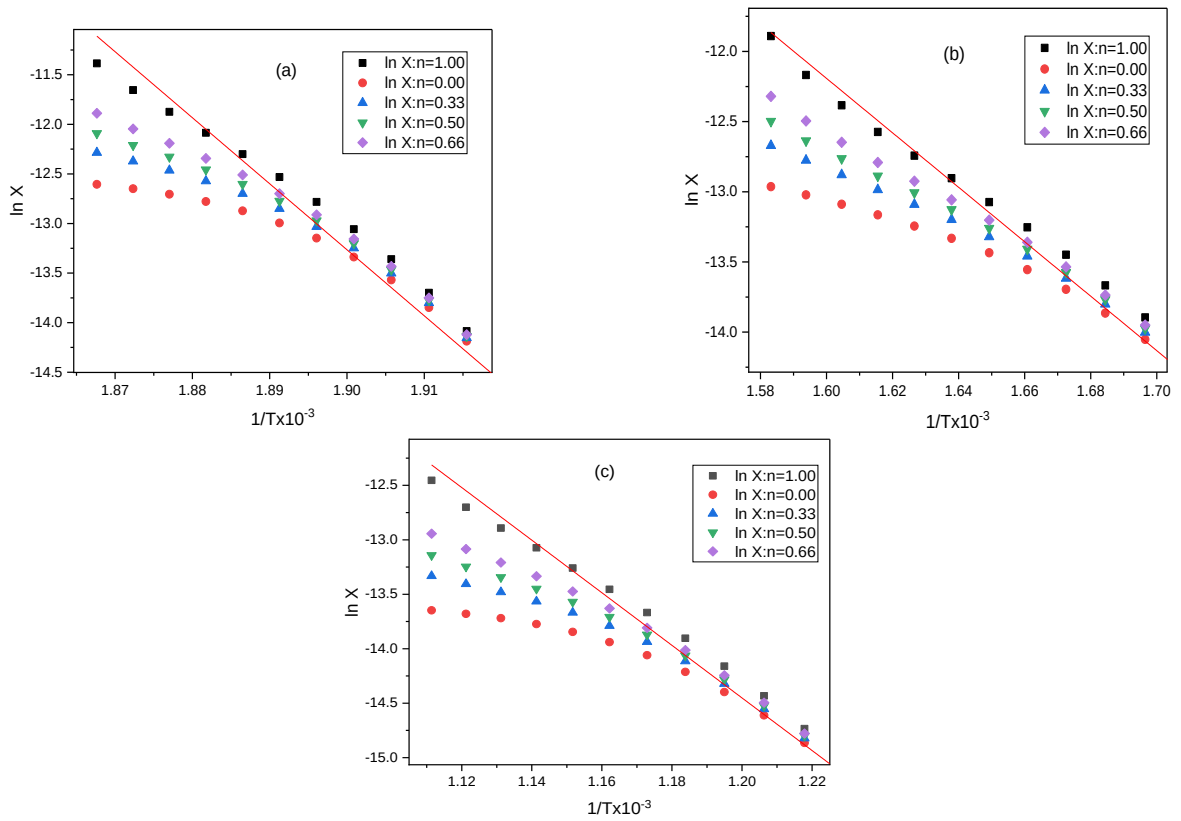

Figure 5 : Coats-Redrern plots of (a) first , (b) second and (c) third degradation steps for $[Pb(HL^1)(H_2O)_2(OAc)]$ complex

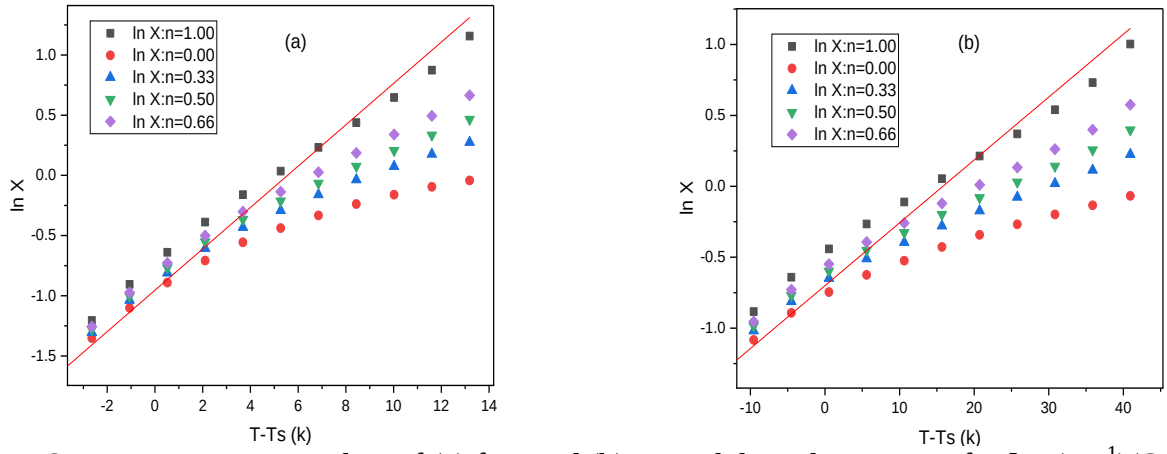

Figure 6: Horowitz-Metzger plots of (a) first and (b) second degradation steps for $[Zn(HL^1)(OAc)]$ complex

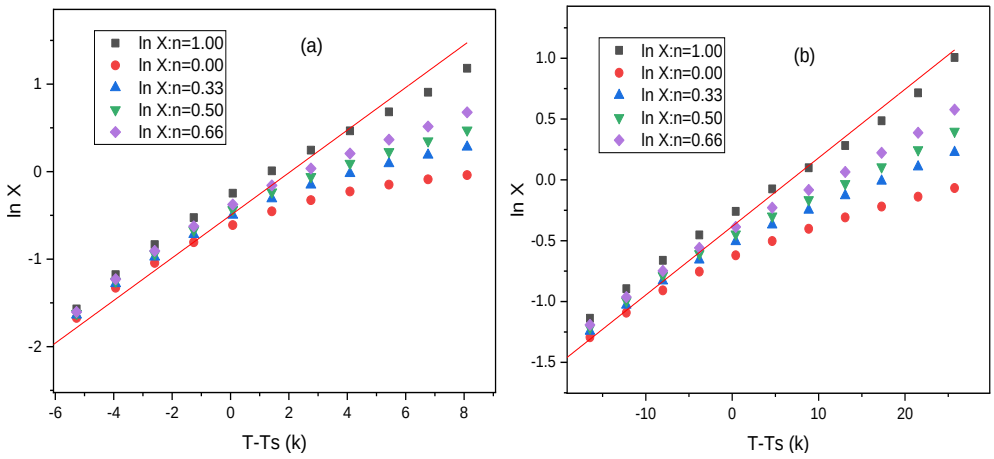

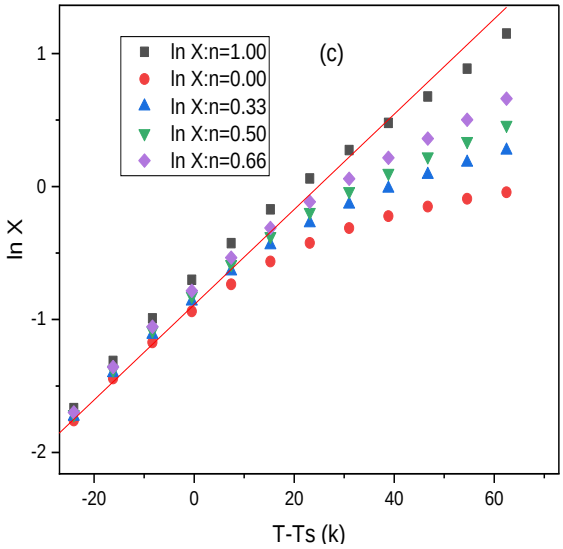

Figure 7: Horowitz-Metzger plots of (a) first , (b) second and (c) third degradation steps for $[Pb(HL^1)(H_2O)_2(OAc)]$ complex.

Table 4: Kinetic Parameters evaluated by Coats-Redfern equation for $[Zn(HL^1)(OAc)]$, $[Pb(HL^1)(H_2O)_2(OAc)]$ complexes

Complex	Step	Mid Temp. (K)	E_a	A (S^{-1})	ΔH^* KJ\mol	ΔS^* KJ\mol	ΔG^* KJ\mol
$[Zn(HL^1)(OAc)]$	First	592.86	497.82	$8.19x10^{41}$	492.89	0.5517	165.77
	Second	716.44	181.95	$7.11x10^{10}$	175.99	-0.0444	207.84
$[Pb(HL^1)(H_2O)_2(OAc)]$	First	527.33	553.61	$1.72x10^{53}$	549.22	0.7695	143.44
	Second	605.92	161.305	$5.3x10^{11}$	156.26	-0.0263	172.23
	Third	837.32	200.73	$8.76x10^{9}$	193.77	-0.0631	246.65

Table 5: Kinetic Parameters evaluated by Horowitz-Metzger equation for $[Zn(HL^1)(OAc)]$, $[Pb(HL^1)(H_2O)_2(OAc)]$ complexes

Complex	Step	Mid Temp. (K)	E_a	A (S^{-1})	ΔH^* KJ\mol	ΔS^* KJ\mol	ΔG^* KJ\mol
$[Zn(HL^1)(OAc)]$	First	592.86	502.14	$1.93\ x10^{42}$	497.21	0.5588	165.86
	Second	716.44	189.11	$2.25\ x10^{11}$	183.15	-0.0348	208.13
$[Pb(HL^1)(H_2O)_2(OAc)]$	First	527.33	562.77	$1.37\ x10^{54}$	558.39	0.7867	143.49
	Second	605.92	172.05	$4.36x10^{12}$	167.02	-0.0088	172.36
	Third	837.32	208.72	$2.58x10^{10}$	201.76	-0.0541	247.12

3.4. Molecular modeling:

3.4.1. Geometry optimization :

The optimized structures and atomic numbers of $[Zn(HL^1)(OAc)]$ and $[Pb(HL^1)(H_2O)_2(OAc)]$ complexes are shown in Figure 8-9. In $[Pb(HL^1)(H_2O)_2(OAc)]$ complex, the bond angles identical to the ones for an octahedral Pb (II) complex with sp^3d^2 hybrid orbitals [24] , while $[Zn(HL^1)(OAc)]$ complex showed tetrahedral geometries.

3.4.2. Global chemical reactivity descriptions

Frontier molecular orbitals (Figures 10, and 11) evaluate kinetic stability, electric optical properties and electronic transitions .The energy gap is used to calculate chemical descriptors such as electronegativity (χ), electrophilicity (ω), hardness (η), chemical potential (μ), and softness (S) of the complexes are assessed based on [25, 26] and the data recorded in (Table 6) where, LUMO is the lowest unoccupied molecular orbital but, HOMO is the highest occupied molecular orbital.

The chemical potential (μ) represents the electrons ability to leave the equilibrium framework, which increases in the subsequent sequence: $[Pb(HL^1)(H_2O)_2(OAc)]$> $[Zn(HL^1)(OAc)]$.

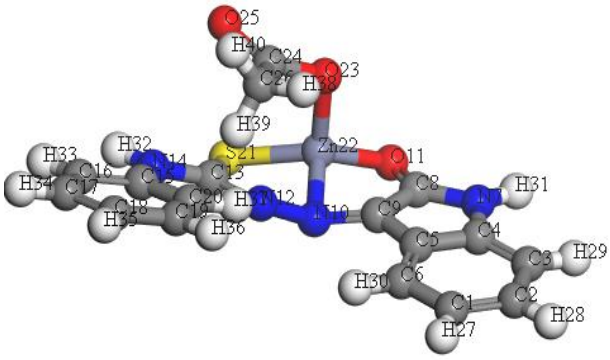

Figure 8: Molecular structure of $[Zn(HL^1)(OAc)]$

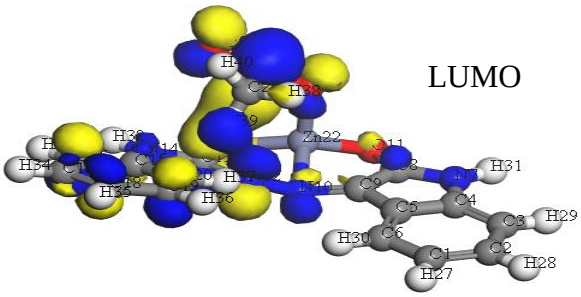

Figure 10: HOMO and LUMO for $[Zn(HL^1)(OAc)]$

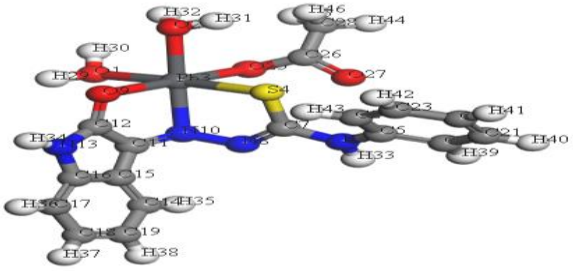

Figure 9 : Molecular structure of $[Pb(HL^1)(H_2O)_2(OAc)]$

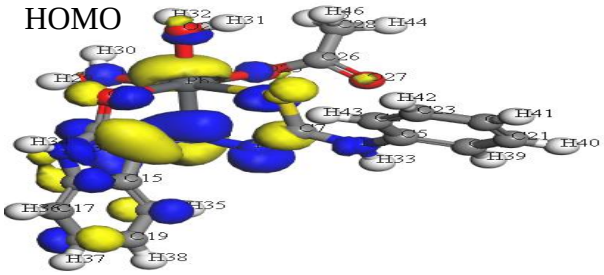

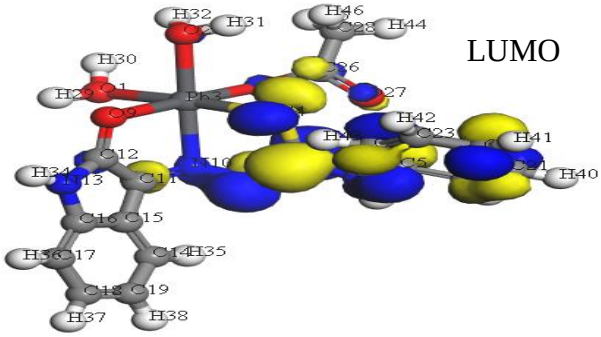

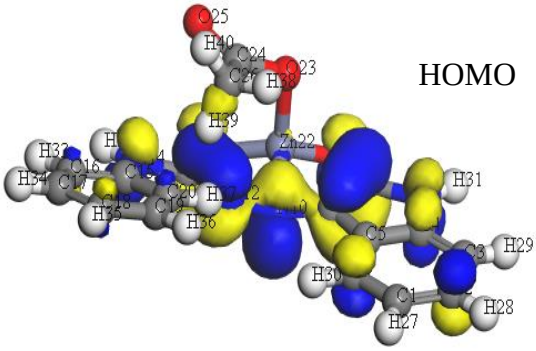

Figure 11 : HOMO and LUMO for $[Pb(HL^1)(H_2O)_2(OAc)]$

Table 6: Calculated E_H, E_L, chemical potential (μ), energy band gap ($E_H - E_L$), electronegativity (χ), global electrophilicity index (ω), global hardness (η), and global softness (S) for $[Zn(HL^1)(OAc)]$ and $[Pb(HL^1)(H_2O)_2(OAc)]$ metal complexes

Compound	E_H (eV)	E_L (eV)	E_H-E_L (eV)	μ (eV)	χ (eV)	η (eV)	S (eV^{-1})	ω (eV)
$[Zn(HL^1)(OAc)]$	-4.380	-2.558	-1.822	-3.469	3.469	0.911	0.4555	6.604808
$[Pb(HL^1)(H_2O)_2(OAc)]$	-4.615	-2.572	-2.043	-3.593	3.593	1.0215	0.5107	6.320726

3.5. Biological potency

3.5.1. Antimicrobial activities :

In-vitro antimicrobial screening of the investigated $[Zn(HL^1)(OAC)]$ and $[Pb(HL^1)(H_2O)_2(OAC)]$ complexes (Table 7) were inspected towards different types of bacteria: gram (+ve) bacteria such as *(Staphylococcus aureus and Bacillus subtilis)* in addition to gram(-ve) bacteria such as *Salmonella typhi* and *Escherichia coli).*Gentamicin used as a standard control in case of antibacterial activity. The following remarks were noticed from the experimental antimicrobial activities:

1- $[Pb(HL^1)(H_2O)_2(OAC)]$ showed no activity against different organisms.

2- In case of *Staphylococcus aureus* the $[Zn(HL^1)(OAC)]$ complex exhibited moderate anti-bacterial activity than the other bacteria.

Table 7: Antimicrobial activity of the investigated [Zn(HL^1)(OAC)] and [Pb(HL^1)(H$_2$O)$_2$(OAC)] complexes represented by inhibitory zone in millimetres(mm)

Samples	Tested organisms							
	E.coli		***Sal.typhi***		***B.subtilis***		***S.aureus***	
	D(mm)	%A.I	D(mm)	%A.I	D(mm)	%A.I	D(mm)	%A.I
[Zn(HL^1)(OAC)]	NA	---	NA	---	NA	---	10	52
[Pb(HL^1)(H$_2$O)$_2$(OAC)]	NA	---	NA	---	NA	---	NA	---
Antibiotic(Gentamicin)	19	100	14	100	19	100	19	100

D: Diameter of inhibition zone (in mm). % A.I.: % Activity index.

3.5.2. DPPH Antioxidant Activity

The compounds Zn(HL^1)(OAC)] and [Pb(HL^1)(H$_2$O)$_2$(OAC)] complexes were examined for their antioxidant activity using DPPH method (Table 8) The results indicated that these compounds expressed antioxidant activities, which were recorded to be concentration dependent. The efficiency of the various tested compounds as antioxidants varied depending on the structure of the compounds. Ascorbic acid used as a reference to compare the compounds' antioxidant activity.

Table 8. DPPH (IC_{50}) of the investigated samples.

Compounds	Ascorbic acid	Zn(II) complex	Pb(II)-complex
IC_{50} (mg/ml)	0.0222	0.047	0.067

4. Conclusion

In this work, we prepared Zn^{2+} and Pb^{2+} complexes derived from *(Z)-2-(2-oxoindolin-3-ylidene)-N-phenylhydrazine-1-carbothioamide* (H$_2$L^1) and characterized by conventional techniques. The DMol3 tool from the material studio program was used to optimize the structures of the H$_2$L^1 ligand and its metal complexes and the [Zn(HL^1)(OAC)] complex are proposed to have a tetrahedral structure and [Pb(L^1)(OAc)(H$_2$O)$_2$] complex have an octahedral structure. From the antimicrobial activities, Zn (II) complex exhibits moderate activity towards *Staphylococcus aureus*. While both complexes show potent antioxidants activity.

5. References

1. Meena, R., et al., (2023) Schiff bases and their metal complexes: Synthesis, structural characteristics and applications, in Schiff Base in Organic, Inorganic and Physical Chemistry., IntechOpen.
2. Schiff, H., (1869) Untersuchungen über salicinderivate. Justus Liebigs Annalen der Chemie,. **150**(2): p. 193-200.
3. Khan, T., et al., (2017) Molecular docking, PASS analysis, bioactivity score prediction, synthesis, characterization and biological activity evaluation of a functionalized 2-butanone thiosemicarbazone ligand and its complexes. *Journal of Chemical Biology*,. **10**(3): p. 91-104.
4. Jindaniya, V., et al., (2024) Synthesis and Diverse Pharmacological Actions of Thiosemicarbazide Analogs: A Review. Letters in Drug Design & Discovery,. **21**(12): p. 2302-2334.
5. Alajroush, D.R., et al., (2024) A comparison of in vitro studies between cobalt (III) and copper (II) complexes with thiosemicarbazone ligands to treat triple negative breast cancer. Inorganica Chimica Acta,. **562**: p. 121898.
6. Castiñeiras, A., et al., (2024) Synthesis, Structural Characterisation, and Electrochemical Properties of Copper (II) Complexes with Functionalized Thiosemicarbazones Derived from 5-Acetylbarbituric Acid. Molecules,. **29**(10): p. 2245.
7. Delgado, G.Y.S. and M. Navarro, (2024) An overview of auric compounds as antimalarial agents and their action against essential targets of the parasite. Coordination Chemistry Reviews,. **503**: p. 215633.
8. Khan, T., et al., (2023) Computational Drug Designing, Synthesis, Characterization and Anti-bacterial Activity Evaluation of Some Mixed Ligand–Metal Complexes of 2-hydroxybenzaldehydethiosemicarbazone as Primary Ligand. Chemistry Africa,. **6**(4): p. 1943-1960.

9. Margalef, J., et al., (2021) Evolution in heterodonor P-N, P-S and P-O chiral ligands for preparing efficient catalysts for asymmetric catalysis. From design to applications. Coordination Chemistry Reviews,. **446**: p. 214120.
10. Mohammed, G.A.A.-K., M.F. Mahmood, and A.-S. Ahmed Jalil, (2022) A Review on Synthesis, Reaction and Biological Importance of Isatin Derivatives. Biomedicine and Chemical Sciences,. **3**(1): p. 193-206.
11. Vogel, A.I., (1961) Quantitative inorganic analysis including elementary instrumental analysis.: Longmans.
12. Abo El-Ata, A.W., et al., (2024) Two New Inner-sphere Pt(II) Thiosemicarbazone Schiff Base Complexes Immobilized into Magnetic Nanoparticles: Synthesis, Characterization, and Biological Investigations. Inorganic Chemistry Communications,. **170**: p. 113366.
13. Bauer, A., et al., (1966*)* Antibiotic susceptibility testing by a standardized single disk method. *American journal of clinical pathology*,. **45**(4_ts): p. 493-496.
14. Mohammed, M.A., et al., (2023*)* Fabrication of novel Fe (III), Co (II), Hg (II), and Pd (II) complexes based on water-soluble ligand (NaH2PH): structural characterization, cyclic voltammetric, powder X-ray diffraction, zeta potential, and biological studies. Applied Organometallic Chemistry,. **37**(1): p. e6910.
15. Yousef, T.A., et al., (2015) Comparative ligational, optical band gap and biological studies on Cr(III) and Fe(III) complexes of hydrazones derived from 2-hydrazinyl-2-oxo-N-phenylacetamide with both vanillin and O-vanillin. Chemical Physics Letters,. **636**: p. 180-192.
16. Belal, D.M., et al., (2023). Fluorescence, cyclic voltammetric, computational, and spectroscopic studies of Mn(II), Co(II), Pd(II), Zn(II) and Cd(II) complexes of salen ligand and their biological applications. *Journal of Molecular Structure*, **1271**: p. 134142.
17. Singh, A., et al., (2014) Manganese (II) and zinc (II) complexes of 4-phenyl (2-methoxybenzoyl)-3-thiosemicarbazide: Synthesis, spectral, structural characterization, thermal behavior and DFT study. Polyhedron,. **73**: p. 98-109.
18. Chandra, K., et al., (1980) Preparation and characterization of carboxylato derivatives of bis-(methyl cyclopentadienyl) titanium(IV). *Journal of Inorganic and Nuclear Chemistry*,. **42**(2): p. 187-193.
19. Nakamoto, K., (1986) Infrared and Raman spectra of inorganic and coordination compounds., New York: Wiley.
20. Maravalli, P. and T. Goudar, (1999*)* Thermal and spectral studies of 3-N-methyl-morpholino-4-amino-5-mercapto-1, 2, 4-triazole and 3-N-methyl-piperidino-4-amino-5-mercapto-1, 2, 4-triazole complexes of cobalt (II), nickel (II) and copper (II). Thermochimica acta,. **325**(1): p. 35-41.
21. Yusuff, K.M. and R. Sreekala, (1990) Thermal and spectral studies of 1-benzyl-2-phenylbenzimidazole complexes of cobalt (II). Thermochimica Acta,. **159**: p. 357-368.
22. Emam, M.E.M., I.M.M. Kenawy, and M.A.H. Hafez, (2001)Study of The Thermal Decomposition of Some New Cyanine Dispersed Dyes. *Journal of Thermal Analysis and Calorimetry*,. **63**(1): p. 75-83.
23. Moore, J.W. and R.G. Pearson, *Kinetics and mechanism*. 1961, New York: John Wiley & Sons.
24. Fetoh, A., et al., (2019*)* Synthesis, characterization, cyclic voltammetry and biological studies of Zn (II), Cd (II), Hg (II) and UO22+ complexes of thiosemicarbazone salt. Applied Organometallic Chemistry,. **33**(4): p. e4787.
25. Padmanabhan, J., et al., (2007) Electrophilicity-based charge transfer descriptor. *J Phys Chem* A,. **111**(7): p. 1358-61.
26. Pearson, R.G., (1988) Absolute electronegativity and hardness: application to inorganic chemistry. Inorganic Chemistry,. **27**(4): p. 734-740.